

SEMI-AUTOMATIC 3D BUILDING EXTRACTION FROM HIGH RESOLUTION SATELLITE IMAGES

Tsend-Ayush Javzandulam, Sooahm Rhee, Taejung Kim

Department of Geoinformatic Engineering, Inha University
253 Yonghyun-dong, Nam-gu, Incheon, 402-751, ROK
javzaa@inha.ac.kr, hsiuyen@inha.ac.kr, tejid@inha.ac.kr

Kyung-Ok Kim

Spatial Information Research Team, Electronics and Telecommunications Research Institute
161 Gajeong-Dong, Yuseong-Gu, Daejeon, 305-350, ROK

ABSTRACT:

Extraction of building is one of essential issues for the 3D city models generation. In recent years, high-resolution satellite imagery has become widely available, and this shows an opportunity for the urban mapping. In this paper, we have developed a semi-automatic algorithm to extract 3D buildings in urban settlements areas from high-spatial resolution panchromatic imagery. The proposed algorithm determines building height interactively by projecting shadow regions for a given building height onto image space and by adjusting the building height until the shadow region and actual shadow in the image match. Proposed algorithm is tested with IKONOS images over Deajeon city and the algorithm showed promising results.

KEY WORDS: Feature extraction, shadow analysis, high-resolution image

1. INTRODUCTION

The generation of 3-D city models is a relevant and challenging task, both from a practical and a scientific point of view and needs of it are increasing. One of essential issues for the 3D city models generation is building extraction. Since high-resolution satellite imagery has become available, and this shows an opportunity for 3D feature extraction.

The objective of this research is to develop an algorithm to extract 3D building from monoscopic high-resolution satellite images. The proposed algorithm works by providing two roof corner points of building. In this study we considered that buildings have uniform height generally descriptive of flat roofs on top of rectangular solids. Walls are considered to be vertical and each building casts its shadow on a surface that is locally flat.

2. ALGORITHM DESCRIPTION

First we provide two opposite roof corner points of a building roof. Using those corner points we then define a region of interest. Then, a line voting process is applied to estimate orientation of a building roof line. After estimated orientation we delineate the whole boundaries of building roof. We then draw the shadow of the building and count overlapping pixels between projected shadow and actual shadow. Here to extract actual shadow region, we applied simple threshold.

2.1 Define a region of interest

We first select two opposite roof corner points $R_1(x_1, y_1)$, $R_2(x_2, y_2)$ of a building roof manually. We need to define ROI which covers any oriented building such that selected two corners to be any two opposite corners of the building roof. We considered that building is rectangular shaped. Therefore if $R_1(x_1, y_1)$, $R_2(x_2, y_2)$ are two opposite points of the building roof, then other two unknown points $R_3(x_3, y_3)$, $R_4(x_4, y_4)$ be on circle with $R_1(x_1, y_1)$ $R_2(x_2, y_2)$ diameter. Those $R_3(x_3, y_3)$, $R_4(x_4, y_4)$ two points be symmetry points for diameter and coordinates of those points be within $[AO]$, $[CO]$ and $[A'O]$, $[C'O]$ intervals (Figure1).

$$R_3(x_3, y_3) : \begin{cases} x_3 \in [A; O] \\ y_3 \in [C; O] \end{cases} \quad (1)$$

$$R_4(x_4, y_4) : \begin{cases} x_4 \in [A'; O] \\ y_4 \in [C'; O] \end{cases} \quad (2)$$

where:

$$O(ox, oy) : \begin{cases} ox = x_1 + \frac{1}{2} \sqrt{(x_1 - x_2)^2} \\ oy = y_1 + \frac{1}{2} \sqrt{(y_1 - y_2)^2} \end{cases}$$

$$A(ax, ay): \begin{cases} ax = x_1 - \frac{1}{2}\sqrt{(x_1 - x_2)^2 + (y_1 - y_2)^2}(1 - \sin \beta) \\ ay = oy \end{cases}$$

$$A'(ax', ay'): \begin{cases} ax' = x_2 + \frac{1}{2}\sqrt{(x_1 - x_2)^2 + (y_1 - y_2)^2}(1 - \sin \beta) \\ ay' = oy \end{cases}$$

$$C(cx, cy): \begin{cases} cx = ox \\ cy = y_1 - \frac{1}{2}\sqrt{(x_1 - x_2)^2 + (y_1 - y_2)^2}(1 - \cos \beta) \end{cases}$$

$$C'(cx', cy'): \begin{cases} cx' = ox \\ cy' = y_2 + \frac{1}{2}\sqrt{(x_1 - x_2)^2 + (y_1 - y_2)^2}(1 - \cos \beta) \end{cases}$$

$$\beta = \arctan\left(\frac{|x_1 - x_2|}{|y_1 - y_2|}\right)$$

Therefore ROI= $ROI(subx, suby)$ be defined as follows:

$$subx = [ax; ax'] \quad suby = [cy, cy'] \quad (5)$$

2.2 Estimate orientation of a building roof and define a building boundaries

After defined ROI, we extract lines from the region of interest we applied the line extraction algorithm proposed by Burns et al (1986). This algorithm defines "line-support regions" by grouping pixels with similar edge orientation and magnitude together and extracts a line from each line support region by planar fitting. After extracted lines we vote the line, which is aligned with the longer side of buildings. A segment of building longer side lines could be defined as shown in Figure2.

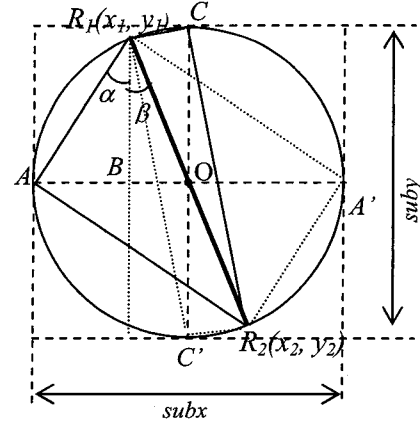


Figure1. Definition of ROI

We then draw the lines from corner point $R_1(x_1, y_1)$ in defined segment (Figure2). In other word, from the point R_1 we draw a lines between γ angles to the horizontal axe and $\gamma + 90^\circ$ to the horizontal axe with angle increment $\Delta\gamma$. Here:

$$\gamma = 90^\circ - \arctan\left(\frac{|y_1 - y_2|}{|x_1 - x_2|}\right) \quad (3)$$

$$\Delta\gamma = 90^\circ - \frac{90^\circ(L-1)}{L} \quad (4)$$

$$L = |y_1 - y_2| * \left(\tan(\varphi) + \frac{1}{\tan(\varphi)} \right)$$

$$\varphi = 45^\circ - \arctan\left(\frac{|y_1 - y_2|}{|x_1 - x_2|}\right)$$

Same time, we draw the lines from corner point $R_2(x_2, y_2)$ in defined range (Figure2) with same $\Delta\gamma$ angle increment. While drawing lines the number of line elements on the each drawn line is counted. Then we select the line with maximum line elements. Since the line is selected will contain more line elements than any other lines along the building orientation, this line will most probably be one of longer side line of building roof. After defined the building orientation ϕ the unknown roof corners $R_3(x_3, y_3)$, $R_4(x_4, y_4)$ could be defined as follows:

$$\begin{cases} x_{3,4} = x_{1,2} \pm \sqrt{(x_1 - x_2)^2 + (y_1 - y_2)^2} \sin \xi \sin \phi \\ y_{3,4} = y_{1,2} \mp \sqrt{(x_1 - x_2)^2 + (y_1 - y_2)^2} \sin \xi \cos \phi \end{cases} \quad (6)$$

where,

$$\xi = \begin{cases} \arctan\left(\frac{|x_1 - x_2|}{|y_1 - y_2|}\right) + \phi - 90^\circ, & \phi \leq 90^\circ \\ \arctan\left(\frac{|x_1 - x_2|}{|y_1 - y_2|}\right) - \phi + 90^\circ, & \phi > 90^\circ \end{cases}$$

ϕ -building orientation angle

Since defined four roof corners points, we can determine building whole boundaries.

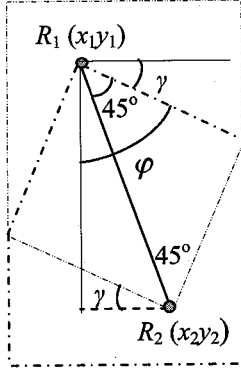


Figure2. Segments of building longer sides

2.3 Draw a shadow line and footprint boundary and get the building height

The initial height of the building is selected as $h=1\text{m}$ or 1 pixels. Since the roof boundaries and height are known, building footprint boundaries can be defined by the azimuth angle and elevation angle of satellite as follows:

$$\begin{cases} px_i^h = rx_i^o + \Delta x_s \\ py_i^h = ry_i^o + \Delta y_s \end{cases} \quad i = \overline{1, BL}$$

$$\Delta y_s = \frac{h}{\tan(El)} \times \sin(Az) \quad (7)$$

$$\Delta x_s = \frac{h}{\tan(El)} \times \cos(Az)$$

where (px_i^h, py_i^h) $i = 1, 2, \dots, BL$ are the points of the building footprint boundaries, h is building height, Az , El are azimuth angle, elevation of satellite respectively.

After determined footprint boundaries, the points of shadow lines (sx_i^h, sy_i^h) $i = 1, 2, \dots, BL$ can be determined by the azimuth angle and elevation angle of sun and it is defined as follows:

$$\begin{cases} sx_i^h = px_i^h + \Delta x_s \\ sy_i^h = py_i^h + \Delta y_s \end{cases} \quad i = \overline{1, BL}$$

$$\Delta x_s = \frac{h}{\tan(SEl)} \times \cos(SAz) \quad (8)$$

$$\Delta y_s = \frac{h}{\tan(SEl)} \times \sin(SAz)$$

where h is building height, SAz , SEl are azimuth angle, elevation of sun respectively. We then draw shadow region while increase the building height by one pixel or one meter. For every step height, we count points of projected shadow lines if all points of line are in actual shadow region. Let us denote those number of counted points at h step height as PN^h . Then this process continues until PN^h reaches 0

$$PN^h = \sum_{i=1}^{BL} Temp_i$$

$$Temp_i = \begin{cases} \sum_{k=1}^{SL} k & \text{if } \forall k : (sx_{i_k}^h, sy_{i_k}^h) \in AS \\ 0 & \text{otherwise} \end{cases} \quad (9)$$

$$SL = \frac{h}{\tan(SEl)}$$

where SL is length of projected shadow line, AS is actual shadow region.

When PN^h reaches 0 the building height is accepted as H , which is maximum value of PN for all h .

$$H : PN^H = \max_h PN^h \quad (10)$$

3. RESULTS AND PERFORMANCE

Ikonos image is used to assess the performance of proposed algorithm. First, employing the proposed building roof extraction algorithm, we extracted 62 building roof lines from 7 regions in the image. Figure3 shows the examples of extracted line image and delineated roof boundaries from an Ikonos image. To verify building orientation by proposed algorithm, we measured the building orientation by manually for the same 62 buildings and we compared result from proposed algorithm to results from manually measurement. The results are shown in Table1. The third column and fourth column of table shows the angular differences and pixel differences in orientation between extracted lines and true

building lines respectively. The average angular error is found that 1.35 degrees or 0.64 pixels. And we extracted 30 building height from 7 sub-regions. Here, we extracted the building height in case whole actual shadow of building is visible and not blocked. Figure4 shows examples of building height extraction. The upper part of figure shows buildings on image before drawing 3D building structure and lower part of image shows drawn structure of building and shadow region.

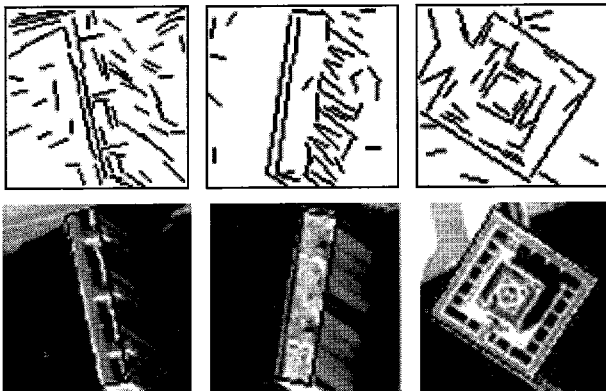


Figure3. Line images (2nd row), Roof boundaries (3rd row)

Table1. The assessment of building roof extraction

Sub-region ID	No of extracted building	Angular error (degrees)	Angular error (pixels)
A	6	1.50	1.22
B	11	1.63	0.54
C	6	1.00	0.44
D	5	0.80	0.34
E	14	1.35	0.61
F	9	0.77	0.36
G	11	1.90	0.90

To verify the results of the building height extraction, using Ikonos stereo pair images we calculated building height manually by measuring tie points on the building and on the ground, by calculating 3D coordinates for the tie points and by calculating the difference between the two. We assumed that building height by stereo analysis is true building height and the extracted building height is compared with building height by stereo analysis.

The difference error of extracted building height and measured building height are shown in Table 2.

The accuracy of the building height extraction is examined using standard error of estimate and it is found that standard error from result of stereo analysis is 1.86 m.

4. CONCLUSIONS

In this study, we proposed an algorithm for extracting roof lines from rectangular-shaped building with a relatively large size. The proposed algorithm gives good result if roof lines are easily detectable and result could be improved by reducing angle increment.

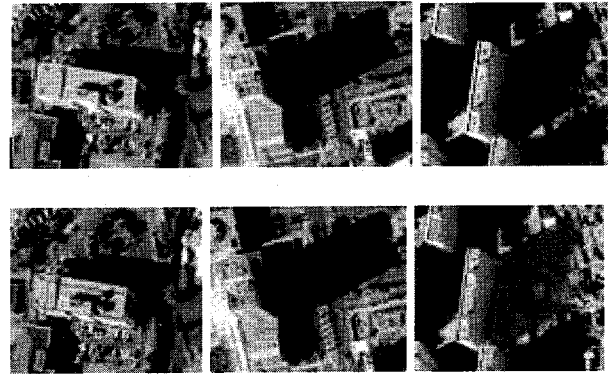


Figure4. Examples of the extracted building height

Table2. The assessment of building height extraction

Sub-region ID	No of extracted building	Difference error between extracted and measured building height (m)
A	5	1.51
B	4	0.62
C	3	0.33
D	3	0.98
E	2	0.60
F	3	1.12
G	10	1.69

5. REFERENCES

- Burns, J. B., A.R. Hanson and E.M. Riseman, 1986. Extracting straight lines, *IEEE Trans. Pattern Analysis and Machine Intelligence*, Vol. 8, pp.425-445.
- Lee, D. S., J. Shan Behal, 2003, Class-Guided Building Extraction from Ikonos imagery, *Photogrammetric Engineering & Remote Sensing*, 69(2), pp 143-150
- Segl, K. and H. Kaufmann, 2001, Detection of Small Objects from High-resolution Panchromatic Satellite Imagery Based on Supervised Image Segmentation, *IEEE Transactions on geoscience and remote sensing*, 39(9) pp20880-2083.
- Kim, T, S. Park, M. Kim, S. Jeong, and Kim.K.O 2004, Semi Automatic Tracking Of Road Centerlines From High Resolution Remote Sensing Data, *Photogrammetric Engineering & Remote Sensing*, 70(12), pp 1417-1422